

On the interpretation of XRISM X-ray measurements of turbulence in the intracluster medium: a comparison with cosmological simulations

F. Vazza^{1,2,*} and G. Brunetti²

¹ Dipartimento di Fisica e Astronomia, Università di Bologna, Via Gobetti 92/3, 40121 Bologna, Italy

² Istituto di Radio Astronomia, INAF, Via Gobetti 101, 40121 Bologna, Italy

Received / Accepted

ABSTRACT

We investigate whether the properties of turbulent gas motions recently measured via X-ray spectroscopy in the Coma cluster of galaxies by XRISM are in tension with the "classical" fluid picture of the intracluster medium on large scales, as produced by a typical high-resolution cosmological simulation. We use a high-resolution simulation of Coma-like cluster of galaxies and show that the Kolmogorov-like turbulence measured in the simulation yields to velocity structure functions and line-width that fully compatible with those measured by the XRISM observation of Coma. These results highlight the combined biases driven by the inhomogeneity of turbulence in the intracluster medium and by the X-ray weighting in observations, and appear to release the tension between the XRISM data and current numerical simulations, showing that a turbulent spectrum much steeper than Kolmogorov is not required by current observational data.

Key words. galaxy: clusters, general – methods: numerical – intergalactic medium – large-scale structure of Universe

1. Introduction

Turbulence in the intracluster medium (ICM) is expected to arise from the stirring associated with the mass growth of clusters (e.g. Norman & Bryan 1999; Subramanian et al. 2006), and may provide pressure support in the atmosphere of clusters of galaxies (e.g. Rasia et al. 2004; Fusco-Femiano & Lapi 2013; Biffi et al. 2016; Eckert et al. 2019). Turbulence may also play a role for the origin of non-thermal components in the ICM, leading to the amplification of magnetic fields (e.g. Dolag et al. 1999; Schekochihin et al. 2005; Cho 2014; Beresnyak & Miniati 2016) and to the re-acceleration of relativistic particles (e.g. Brunetti et al. 2004; Cassano & Brunetti 2005; Brunetti & Lazarian 2016; Beduzzi et al. 2024; Nishiwaki et al. 2024). The turbulence in clusters of galaxies has been since long studied with cosmological hydrodynamical simulations (e.g. Norman & Bryan 1999; Dolag et al. 2005; Iapichino & Niemeyer 2008; Vazza et al. 2011; Miniati 2014), albeit its precise determination depends on the specific algorithms used to filter out bulk motions, shocks and other perturbations from the 3-dimensional velocity field (e.g. see discussion in Vazza et al. 2012; Nelson et al. 2014; Vazza et al. 2017, 2018a; Angelinelli et al. 2020).

Both X-ray and Sunyaev-Zeldovich surface brightness fluctuations observed in clusters were interpreted as indications of moderate density/pressure fluctuations induced by turbulence (e.g. Schuecker et al. 2004; Churazov et al. 2012; Gaspari & Churazov 2013; Zhuravleva et al. 2012; Khatri & Gaspari 2016; Eckert et al. 2019; Dupourqué et al. 2024). On the other hand, the direct measurement of turbulence in the ICM has only since recently become possible, with spectroscopic X-ray observations of a few clusters. The Hitomi satellite managed to detect root-

mean square velocities in the (fairly relaxed) Perseus cluster of ~ 200 km/s on ≤ 60 kpc (e.g. Hitomi Collaboration et al. 2016; ZuHone et al. 2018). More recently, the XRISM collaboration reported first measurements of bulk velocity and of the velocity dispersion along a few lines of sight (LOS) crossing three galaxy clusters in the local Universe: A2029 (XRISM Collaboration et al. 2025; Xrism Collaboration et al. 2025), Coma (XRISM Collaboration et al. 2025a), Centaurus (XRISM Collaboration et al. 2025b). In all cases, the reported values of LOS velocity dispersion (once converted into three-dimensional values, assuming isotropic velocity distributions) are in the $\sim 200 - 300$ km/s range at all radii, resulting in typical inferred kinetic to total pressure support of $\sim 2 - 3\%$, naively resulting in a much smaller estimate than in previous simulations. A key finding obtained by XRISM in the case of the Coma cluster (a massive perturbed system hosting multiple diffuse radio emissions, Bonafede et al. 2021 for recent observations) is that velocity structure function of gas motions is much steeper than the baseline expectation from Kolmogorov theory, possibly due to either a very large effective viscosity in the ICM inducing a large dissipation scale of turbulent motions, or a situation where large scale motions generated by recent mergers have not yet cascaded down to small scales (XRISM Collaboration et al. 2025a). If confirmed, these findings would start providing fundamental insights on the properties of turbulence in the ICM and on the role of collision-less effects. Indeed in a weakly-collisional plasma instabilities driven by large scale motions may govern the effective viscosity of the plasma and the fraction of the energy that is drained from large scales into small scale turbulence (e.g. Kunz et al. 2011; Brunetti & Lazarian 2011; Rincon et al. 2016; St-Onge & Kunz 2018; St-Onge et al. 2020; Kempf & Rincon 2025).

* e-mail: franco.vazza2@unibo.it

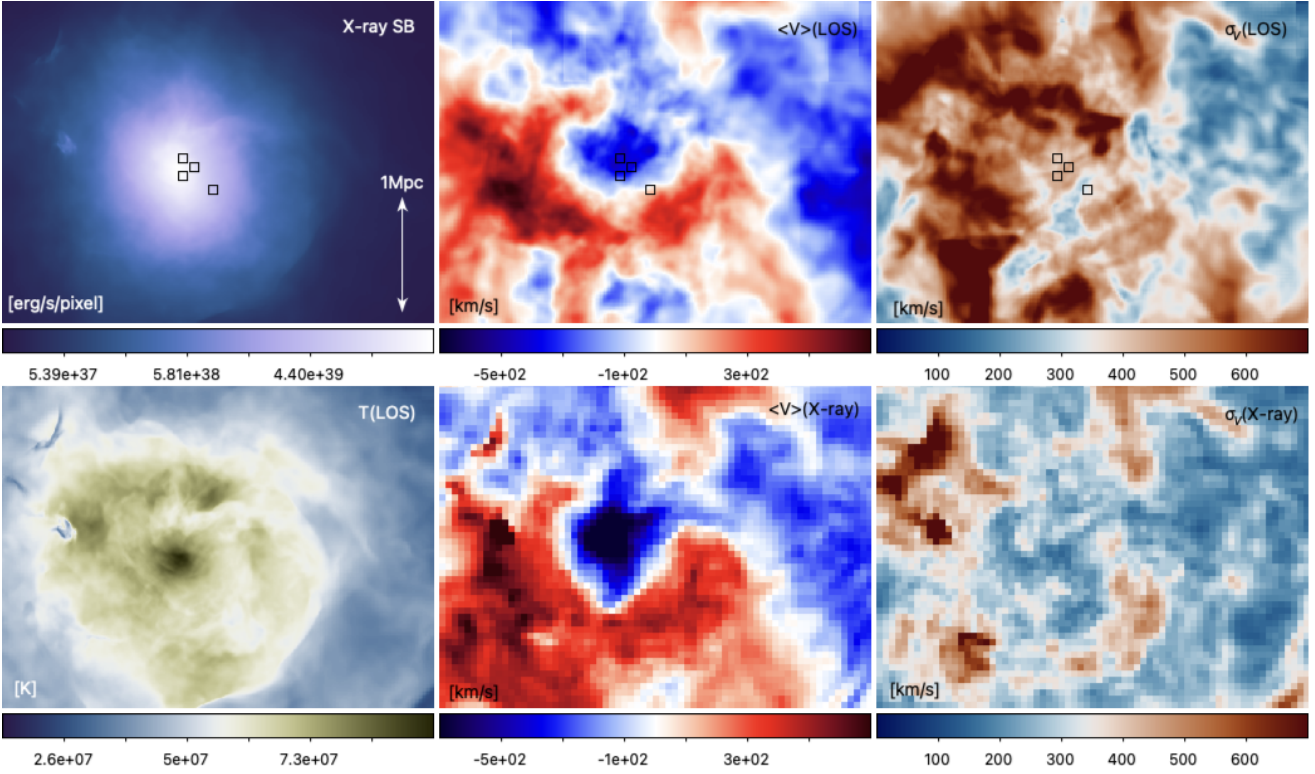


Fig. 1. Projected X-ray surface brightness in the [5–7] keV energy range for our simulated cluster (top left), average X-ray weighted gas temperature (lower left), average gas velocity along the line of sight, either using a volume-weighting procedure (top centre) or an X-ray emissivity weighting along the line of sight, within pixel of 90×90 kpc² to mimic XRISM field of view for Coma (bottom centre). Gas velocity dispersion along the line of sight, again either using a volume-weighting procedure (top right) or an X-ray emissivity weighting along the line of sight, for 90×90 kpc² pixels (bottom right). The black squares refer to the regions used to produce the line emission profiles given in Fig. 3.

Given the potential impact of these findings, in this article we attempt to explore how effective the current XRISM measurements really are in obtaining constraints on the turbulence in the ICM and whether they are really in disagreement with current cosmological simulations which are based on a purely collisional model of the ICM. The paper is structured as follows: in Sec. 2 we describe our simulation; in Sec. 3 we give our results and in Sec. 4 we discuss the implications of this work for the interpretation of existing and future observations.

2. Methods

We analyse a high-resolution cluster simulation obtained with the Eulerian code ENZO (Bryan et al. 2014), already used by our group in previous work (e.g. Vazza et al. 2018b; Domínguez-Fernández et al. 2019; Bonafede et al. 2021). This ideal MHD simulation used up to eight levels of Adaptive Mesh Refinement (AMR) to reach a peak spatial resolution of $\Delta x = 3.95$ kpc/cell in most of the cluster core, and a resolution of $\Delta x = 15.8$ kpc/cell in the entire virial volume (Vazza et al. 2018b). We choose this cluster in particular because our previous work showed that it has: i) a total mass similar to the real Coma cluster ($M_{200} \approx 1.1 \cdot 10^{15} M_{\odot}$ at $z = 0.02$); ii) a turbulent kinetic pressure (within a ~ 300 kpc scale) estimated to be $\sim 5\%$ of the total pressure in the innermost Mpc³; iii) a profile of Faraday Rotation compatible with the real one observed in Coma (Bonafede et al. 2013), arising from the small-scale dynamo turbulent amplification of an initial 0.1 nG seed field (Vazza et al. 2018b); iv) a simulated synchrotron radio power, assuming reacceleration of electrons by the turbulence in the cluster, based on a Fermi II adiabatic stochastic acceleration

model (e.g. Brunetti & Lazarian 2016), compatible with the real emission from Coma (Bonafede et al. 2021). To compare with XRISM observations, we computed the continuum and line X-ray emission from all cells in the simulation within the [5, 7] keV energy range, assuming a constant composition and metallicity (30% of the solar one) for all cells, with the B-APEC emission model (<https://heasarc.gsfc.nasa.gov/xanadu/xspec/manual/Models.html>). For our analysis, we also had to identify the turbulent part of the 3-dimensional gas velocity field in the ICM, with a small-scale filtering approach, based on previous work (Vazza et al. 2006, 2009, 2011, 2012, 2017; Angelinelli et al. 2020; Simonte et al. 2022). While more complex approaches using a variable filtering length, combined with the masking of shocks can be used for a more accurate removal (Vazza et al. 2012; Angelinelli et al. 2020; Valdarnini 2019), our previous work showed that setting $\Lambda_t = 300$ kpc gives a robust enough separation between large-scale bulk motions and smaller scales isotropic turbulent motions in $\sim 10^{15} M_{\odot}$ clusters. Therefore in the remainder of this paper we estimate of the 3-dimensional turbulent velocity field is given by $\delta \mathbf{v} = \mathbf{v} - \langle \mathbf{v} \rangle_{\Lambda_t}$, where \mathbf{v} is the local velocity and density and $\langle \mathbf{v} \rangle_{\Lambda_t}$ is the velocity averaged within Λ_t .

3. Results

We give in Figure 1 the maps of projected X-ray surface brightness obtained in the [5–7] keV band, of the X-ray weighted mean gas temperature, and of the total velocity and velocity dispersion along the line of sight. The latter two are computed in two ways: a) in the top panels, by directly computing the average (volume-weighted) velocity and velocity dispersion along each the LOS,

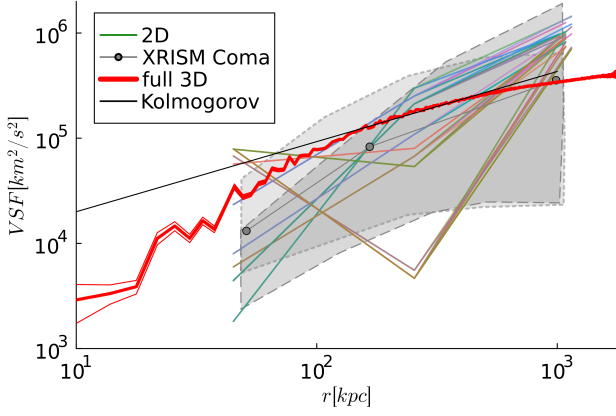


Fig. 2. Coloured lines: simulated VSFs using 50 random extractions of 2D measurements of the velocity field along the LOS in $90 \times 90 \text{ kpc}^2$ pixels, with similar separations as in the XRISM observation of Coma. Red line with error bars: full 3-dimensional VSF for the velocity along the line of sight component, using 10^7 cells in the cluster volume. The points are the XRISM measurements for Coma, while the grey shaded areas show include the 68% cosmic variance uncertainty and the measurement statistical errors on their measure.

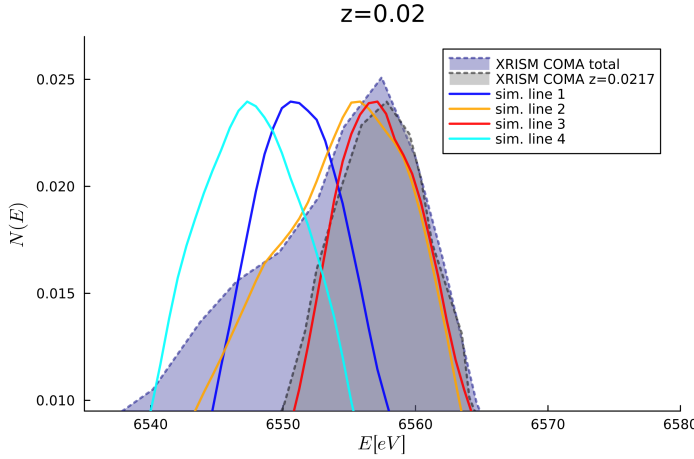


Fig. 3. Simulated line profiles for the four FOVs indicated in Fig. 1 (color lines) compared with the reconstructed line models for the XRISM observation of the Coma cluster produced by XRISM Collaboration et al. (2025a), given by the two shaded areas.

considering a field of view $3.95 \times 3.95 \text{ kpc}^2$ for each LOS (as in the original resolution of the simulation), or b) by computing the X-ray emission-weighted average velocity and velocity dispersion along the LOS after resampling on $90 \times 90 \text{ kpc}^2$ pixels (corresponding to a XRISM FOV at the distance of the Coma cluster), similar to XRISM Collaboration et al. (2025a).

A key finding by XRISM Collaboration et al. (2025a) we wish to study is that their measured velocity structure function (VSF) is much steeper than expected from the Kolmogorov model of turbulence, which on the other hand is a general finding of cosmological simulations (Dolag et al. 2005; Vazza et al. 2009, 2011, 2017; Simonte et al. 2022). This conclusion is based on the combination of the measured VSF and width of the emission lines, because a Kolmogorov model fitting the measured VSF would predict a line more than twice wider than the measured one. The VSF is defined as $VSF(\mathbf{r}) = \langle |\mathbf{v}_z(\chi) - \mathbf{v}_z(\chi + \mathbf{r})|^2 \rangle$, where \mathbf{v}_z is the velocity along the line of sight and \mathbf{r} is a displacement with respect to the χ position. The Kolmogorov model predicts a $VSF(r) \propto r^{2/3}$ scaling for isotropic and volume-filling

turbulence. Our simulation allows us to measure, both, the VSF in 3-dimensions and in the projected information of the velocity maps of Fig. 1. Figure 2 gives the 3-dimensional VSF for the velocity component along the LOS, computed from 10^7 cells in the cluster volume. In line with previous work (e.g. Vazza et al. 2011, 2017; Simonte et al. 2022), for roughly two orders of magnitude in spatial scales the measured VSF is in line with the Kolmogorov model ($\propto r^{2/3}$).¹ To mimic the recent XRISM analysis of Coma, we produced 50 random variations of the 2D estimates of the VSF, based on the X-ray weighted velocity map with $90 \times 90 \text{ kpc}^2$ pixels (as in the last column of Fig. 1). In detail, we used triplets of random pixels with a relative projected distance as in the real observation, and we built their VSF by computing the velocity difference between them. The results are shown by the multitude of thin coloured lines (some of which producing even inverted trends of the VSF with increasing scale) in Fig. 2, which are over-imposed to the actual XRISM data point (grey points) and to the region of uncertainties given by the two models $VSF(r) \propto r^{2/3}$ or $\propto r^6$ discussed in XRISM Collaboration et al. (2025a). Within the large scattered distribution of randomly measured VSFs, a large fraction of them are similar to the recent XRISM measurement, and within their estimated statistical uncertainty and cosmic variance. This test shows that our simulated Coma-like cluster is characterized by a 3-dimensional velocity field which essentially is Kolmogorov-type turbulence in a stratified atmosphere, and that its observable VSFs are in principle compatible with the measurements recently made with XRISM. Next, we show that the same simulated velocity field also appears capable to reproduce the iron line emission measured by XRISM. In detail, we simulated the iron line emission from four lines randomly drawn within a $\leq 200 \text{ kpc}$ region from the cluster centre (whose position is shown by the black squares in Fig. 1), as shown in Fig. 3. The line emission profile is generated by adding the X-ray emission in the [5-7]keV band for each cell along the line of sight (assuming a constant metallicity) and by including the $\Delta E/E = v_z/c$ Doppler shift of the line centre, based on the measured velocity along the LOS (again for $90 \times 90 \text{ kpc}^2$ FOV). The additional shaded areas show the best models produced to fit the North-West quadrant of the XRISM observation of Coma, which plausibly includes a bulk motion along the line of sight. Our simulated FOVs generate line shapes with a range of profiles, including cases which closely match the Iron line profile measured by XRISM on Coma (like line 3 for the $z = 0.0217$ component in the Coma observation, or line 2 for the additional velocity component detected by XRISM along the LOS), while other have different shapes (e.g. lines 1 and 4). This might seem at odds with the conclusions in XRISM Collaboration et al. (2025a), where a Kolmogorov model matching the observed VSF results in a line width that is too large compared to observations. A hint for the discrepancy is that in their procedure, homogenous Kolmogorov turbulence and a β -model gas distribution are assumed, while instead turbulence in our simulated cluster is far from homogeneous (e.g. see Fig. 1), and turbulent regions cover only a fraction of the volume. As a crucial consequence, the effective line width is reduced compared to that estimated from a simpler homogeneous conditions. It shall be noticed that this result appears in line with the test shown in the Appendix of XRISM Collaboration et al. (2025a),

¹ There is a known hint of a small steepening on small scales, interpreted as an effect of the ICM stratification, combined with the effect of numerical dissipation on small-scales (e.g. see discussion in Simonte et al. 2022).

where the emission-weighted velocity dispersion for 14 Coma-like clusters is measured.

Next, we perform a more systematic analysis of the entire simulated velocity map. The top panel of Figure 4 gives the distribution of the X-ray weighted velocity dispersion and of the distribution of "true" turbulence along the line of sight, based on our fiducial 3-dimensional small-scale filtering procedure, while the central panel gives the ratio between the two within each 90×90 kpc² lines of sight. In both cases we consider only central (≤ 500 kpc from the cluster centre) regions. While the distribution of the X-ray velocity dispersion is well within the estimates recently produced by XRISM Collaboration et al. (2025a), the distribution of our best estimate of the true turbulent content in the same cluster is higher on average, typically by $\sim 40 - 50\%$ (at a $\sim 200 - 300$ kpc radius). The lower panel gives the ratio between the X-ray weighted and the true turbulent velocity dispersion as a function of the X-ray emission within FOV: the ratio on average decreases as a function of increasing X-ray surface brightness albeit with a significant scatter which does not allow to extract a simple correction factor, because the mismatch does not only depend on the X-ray surface brightness, but rather on the specific gas structures along the LOS.

Finally, we re-assess the amount of the non-thermal pressure support in this cluster, to closely compare with the result by XRISM Collaboration et al. (2025a), who reported a kinetic pressure support $\approx 3\%$ of the total pressure in the cluster centre. In Figure 5 we give the 3-dimensional profile of the ratio between turbulent and total pressure within the radius. We use the same formula by XRISM Collaboration et al. (2025a): $p_{\text{turb,kin}}/p_{\text{tot}} = [1 + 3/(\gamma M_{3D}^2)]^{-1}$ where M_{3D} is the local 3-dimensional Mach number measured by dividing either the turbulent velocity dispersion or the total velocity dispersion for the sound speed of each cell. In both cases the non-thermal pressure ratio increases with radius, as expected (Vazza et al. 2018a), with the total (unfiltered) kinetic pressure ratio being up to ~ 5 times higher than the isotropic turbulent one. The latter is in all cases higher than what is estimated for the Coma cluster by XRISM Collaboration et al. (2025a), and it reaches $\sim 5\%$ within 1.5 Mpc from the cluster centre, which is $\approx R_{500}$ for this cluster. This is in line with our previous estimates for this, and similar simulated clusters (e.g. Vazza et al. 2011, 2018b), and it represents a lower limit on the turbulent budget of the cluster, which may also comprise larger scale anisotropic motions (e.g. Vazza et al. 2018a; Angelinelli et al. 2020). Based on the relative distribution between X-ray weighted and true turbulence along the line of sight, we conclude that actual turbulent non-thermal support in the ICM is significantly higher (typically by a factor ~ 2) than the estimate given by spectroscopic X-ray analysis, which is in turn biased low by the smaller range of scales sampled through X-ray emission.

4. Conclusions

The physics of turbulence in the weakly collisional intracluster medium is expected to be more complicated than that in fluid numerical simulations, where an idealised collisional plasma is assumed. In this article we have investigated whether the recently observed properties of turbulent gas motions inferred via X-ray spectroscopy by XRISM Collaboration et al. (2025a) are already in tension with the idealised view from numerical simulations on large scales (≥ 10 kpc) and have already started to pinpoint aspect driven by the collisionless nature of the intra-cluster medium, which are expected to arise on smaller scales (e.g. Kunz et al. 2011; Brunetti & Lazarian 2011; Santos-Lima

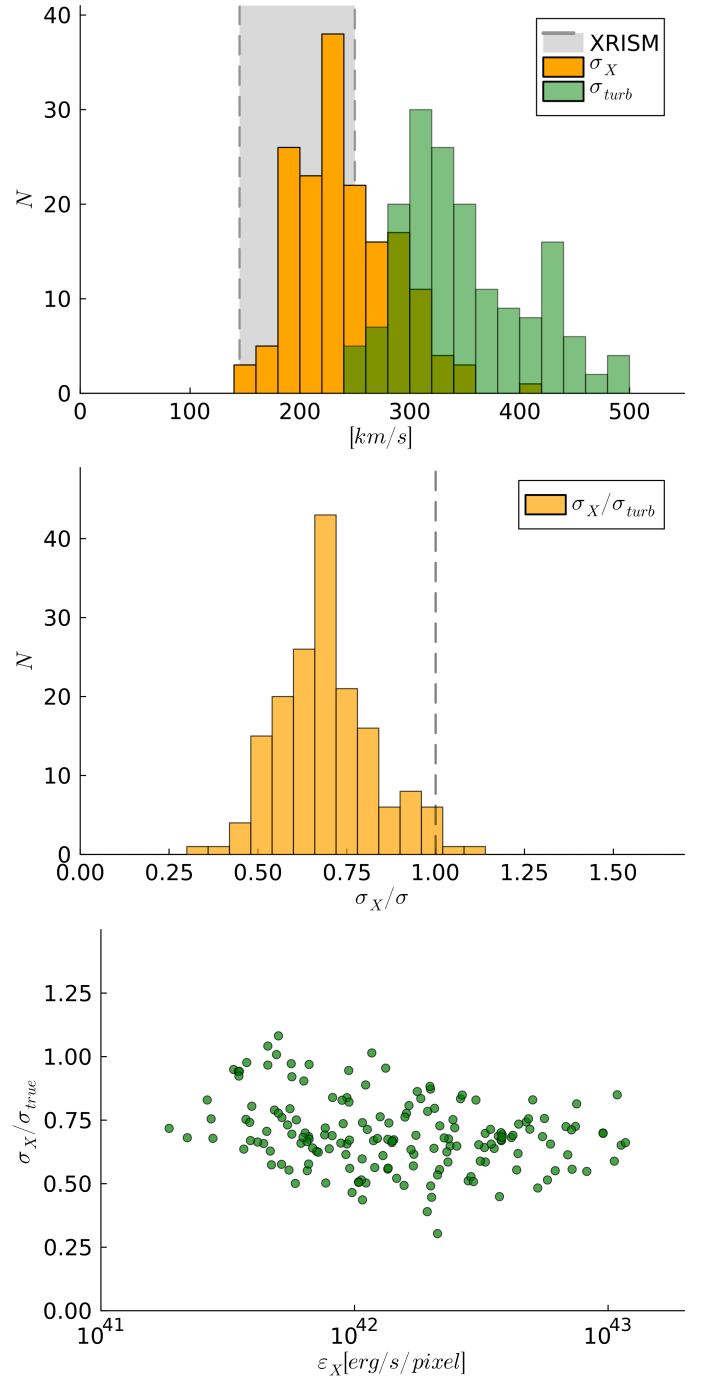


Fig. 4. Top panel: histograms of X-ray weighted velocity dispersion along the LOS and of volume weighted velocity dispersion for 90×90 kpc² pixels maps. The additional vertical lines give the values inferred for the central FOVs observed by XRISM in the central region of Coma. Central panel: histograms for the ratio between the two estimates of the velocity dispersion above, either for the core cluster region (green) or for the full cluster volume (orange). Bottom panel: relation between the ratio of the volume weighted and the X-ray weighted velocity dispersion as a function of the X-ray emission of cells.

et al. 2014; Brunetti & Jones 2014; Rincon et al. 2016; St-Onge & Kunz 2018; St-Onge et al. 2020; Kempf & Rincon 2025).

In particular, using a typical high-resolution cosmological simulation of a Coma-like cluster of galaxies (Sec.2), we have shown that:

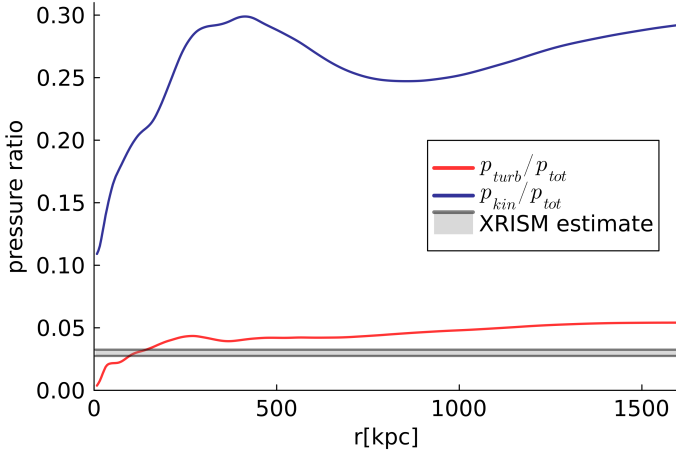


Fig. 5. 3-dimensional radial profile of the non-thermal to total pressure ratio within the radius, considering our fiducial estimate of isotropic turbulence (via small-scale filtering within $\Lambda = 300$ kpc, p_{turb}), or the total (unfiltered) gas velocity field (p_{kin}). The horizontal grey strip give the estimate for the Coma cluster by XRISM Collaboration et al. (2025a).

- spectroscopic X-ray estimates of the ICM turbulence along the LOS are likely to be biased towards the X-ray brightest X-ray portion of the ICM volume, which produce an underestimate (overall by a $\sim 50\%$ factor on average, compared to the energy weighted turbulent dispersion along the LOS) due to two factors: the limited range of scales of the turbulent spectrum sampled in this way, and the limited radial extent from the cluster centre which can be probed by X-ray observations (which are biased towards the innermost dense cluster regions).
- The fact that turbulent energy and X-ray emission only loosely correlate in the ICM, explains why the total turbulent kinetic pressure support in our Coma-like cluster of galaxies is $\sim 5\%$ of the total pressure (or up to 25% if the full unfiltered kinetic energy is considered), even if our simulated X-ray line broadening is consistent with the observation by XRISM Collaboration et al. (2025a). The actual turbulent pressure support in the ICM can plausibly higher than what is estimated from X-ray spectroscopy, although it is not possible to derive a simple correction factor, due to the large measured scatter in the relation between the true and the X-ray weighted turbulent dispersion along the LOS (see also, e.g. Roncarelli et al. 2018; Biffi et al. 2022, for valuable numerical work on this issue).
- The velocity structure function of gas motions in the simulated ICM is well in line with Kolomogorov turbulence in a stratified atmosphere, and consistent with the last two decades of numerical simulation. Nevertheless, our tests show that if the VSF is estimated just using a limited set of FOV from X-ray observations, the resulting VSF is too affected by statistical uncertainties to be a reliable proxy of turbulent properties.

In summary, we suggest that the fluid turbulence typically produced by cosmological simulations of clusters in the literature is compatible with the latest XRISM measurements in Coma (and possibly in other clusters), once that the realistic degree of non-homogeneity of the ICM, the multi-scale nature of the ICM turbulent flows and the biases inherent to X-ray spectroscopy are taken into account. This appear enough to release the tension between the XRISM data and current numerical simulations, and it

shows that a turbulent spectrum much steeper than Kolmogorov is not required by current data.

acknowledgements

FV has been partially supported by Fondazione Cariplo and Fondazione CDP, through grant n° Rif: 2022-2088 CUP J33C22004310003 for the "BREAKTHRU" project. F.V. acknowledges the CINECA award "IsC4_FINRADG" under the ISCR initiative, for the availability of high-performance computing resources and support.

References

- Angelinelli, M., Vazza, F., Giocoli, C., et al. 2020, MNRAS, 495, 864
 Beduzzi, L., Vazza, F., Cuciti, V., et al. 2024, arXiv e-prints, arXiv:2406.09859
 Beresnyak, A. & Miniati, F. 2016, ApJ, 817, 127
 Biffi, V., Borgani, S., Murante, G., et al. 2016, ApJ, 827, 112
 Biffi, V., Zuhone, J. A., Mroczkowski, T., Bulbul, E., & Forman, W. 2022, A&A, 663, A76
 Bonafede, A., Brunetti, G., Vazza, F., et al. 2021, ApJ, 907, 32
 Bonafede, A., Vazza, F., Brüggen, M., et al. 2013, MNRAS, 433, 3208
 Brunetti, G., Blasi, P., Cassano, R., & Gabici, S. 2004, MNRAS, 350, 1174
 Brunetti, G. & Jones, T. W. 2014, International Journal of Modern Physics D, 23, 1430007
 Brunetti, G. & Lazarian, A. 2011, MNRAS, 412, 817
 Brunetti, G. & Lazarian, A. 2016, MNRAS, 458, 2584
 Bryan, G. L., Norman, M. L., O'Shea, B. W., et al. 2014, ApJS, 211, 19
 Cassano, R. & Brunetti, G. 2005, MNRAS, 357, 1313
 Cho, J. 2014, ApJ, 797, 133
 Churazov, E., Vikhlinin, A., Zhuravleva, I., et al. 2012, MNRAS, 421, 1123
 Dolag, K., Bartelmann, M., & Lesch, H. 1999, A&A, 348, 351
 Dolag, K., Vazza, F., Brunetti, G., & Tormen, G. 2005, MNRAS, 364, 753
 Domínguez-Fernández, P., Vazza, F., Brüggen, M., & Brunetti, G. 2019, MNRAS, 486, 623
 Dupourqué, S., Clerc, N., Pointecouteau, E., et al. 2024, A&A, 687, A58
 Eckert, D., Ghirardini, V., Ettori, S., et al. 2019, A&A, 621, A40
 Fusco-Femiano, R. & Lapi, A. 2013, ApJ, 771, 102
 Gaspari, M. & Churazov, E. 2013, A&A, 559, A78
 Hitomi Collaboration, Aharonian, F., Akamatsu, H., et al. 2016, Nature, 535, 117
 Iapichino, L. & Niemeyer, J. C. 2008, MNRAS, 388, 1089
 Kempf, J. M. & Rincon, F. 2025, A&A, 694, A25
 Khatri, R. & Gaspari, M. 2016, MNRAS, 463, 655
 Kunz, M. W., Schekochihin, A. A., Cowley, S. C., Binney, J. J., & Sanders, J. S. 2011, MNRAS, 410, 2446
 Miniati, F. 2014, ApJ, 782, 21
 Nelson, K., Lau, E. T., & Nagai, D. 2014, ApJ, 792, 25
 Nishiwaki, K., Brunetti, G., Vazza, F., & Gheller, C. 2024, ApJ, 961, 15
 Norman, M. L. & Bryan, G. L. 1999, in Lecture Notes in Physics, Berlin Springer Verlag, Vol. 530, The Radio Galaxy Messier 87, ed. H.-J. Röser & K. Meisenheimer, 106+
 Rasia, E., Tormen, G., & Moscardini, L. 2004, MNRAS, 351, 237
 Rincon, F., Califano, F., Schekochihin, A. A., & Valentini, F. 2016, Proceedings of the National Academy of Science, 113, 3950
 Roncarelli, M., Gaspari, M., Ettori, S., et al. 2018, A&A, 618, A39
 Santos-Lima, R., de Gouveia Dal Pino, E. M., Kowal, G., et al. 2014, ApJ, 781, 84
 Schekochihin, A. A., Cowley, S. C., Kulsrud, R. M., Hammett, G. W., & Sharma, P. 2005, ApJ, 629, 139
 Schuecker, P., Finoguenov, A., Miniati, F., Böhringer, H., & Briel, U. G. 2004, A&A, 426, 387
 Simonte, M., Vazza, F., Brighenti, F., et al. 2022, A&A, 658, A149
 St-Onge, D. A. & Kunz, M. W. 2018, ApJ, 863, L25
 St-Onge, D. A., Kunz, M. W., Squire, J., & Schekochihin, A. A. 2020, Journal of Plasma Physics, 86, 905860503
 Subramanian, K., Shukurov, A., & Haugen, N. E. L. 2006, MNRAS, 366, 1437
 Valdarnini, R. 2019, ApJ, 874, 42
 Vazza, F., Angelinelli, M., Jones, T. W., et al. 2018a, MNRAS, 481, L120
 Vazza, F., Brunetti, G., Brüggen, M., & Bonafede, A. 2018b, MNRAS, 474, 1672
 Vazza, F., Brunetti, G., Gheller, C., Brunino, R., & Brüggen, M. 2011, A&A, 529, A17+
 Vazza, F., Brunetti, G., Kritsuk, A., et al. 2009, A&A, 504, 33
 Vazza, F., Jones, T. W., Brüggen, M., et al. 2017, MNRAS, 464, 210
 Vazza, F., Roediger, E., & Brüggen, M. 2012, A&A, 544, A103
 Vazza, F., Tormen, G., Cassano, R., Brunetti, G., & Dolag, K. 2006, MNRAS, 369, L14
 XRISM Collaboration, Audard, M., Awaki, H., et al. 2025, arXiv e-prints, arXiv:2505.06533
 Xrism Collaboration, Audard, M., Awaki, H., et al. 2025, ApJ, 982, L5
 XRISM Collaboration, Audard, M., Awaki, H., et al. 2025a, arXiv e-prints, arXiv:2504.20928
 XRISM Collaboration, Audard, M., Awaki, H., et al. 2025b, Nature, 638, 365
 Zhuravleva, I., Churazov, E., Kravtsov, A., & Sunyaev, R. 2012, MNRAS, 422, 2712
 Zuhone, J. A., Miller, E. D., Bulbul, E., & Zhuravleva, I. 2018, ApJ, 853, 180